**Proceedings of ASME FEDSM'01**
**2001 ASME Fluids Engineering Division Summer Meeting**
**New Orleans, Louisiana, May 29- June 1, 2001**

**FEDSM2001-18037**

# SPECIAL ULTRASONIC FLOWMETERS FOR IN-SITU DIAGNOSIS OF SWIRL AND CROSS FLOW

T. T. Yeh and P. I. Espina
Fluid Flow Group
National Institute of Standards and Technology
Gaithersburg, Maryland 20899
USA

## ABSTRACT

The presence of non-ideal flow profiles is known to cause significant metering inaccuracies in conventional pipelines. The characteristics of secondary flows are also important for mixer design where flow non-ideality is highly desired. Advances in ultrasonic technology and computing capabilities offer prospects for detecting secondary flows in pipelines and improving flow meter performance. This paper describes ultrasonic flow measurements made using dual-sensor, travel-time techniques. Multi-reflection flow meters in circular pipe are discussed in detail. Depending on the sensor and acoustic path arrangements, ultrasonic flow meters can be designed to measure different flow velocity components.

Conventional ultrasonic flow meters, having sensors located at both downstream and upstream positions, are used to measure the flow. This work evaluates the prospects of performing non-ideal secondary flow measurement. The sensors and the acoustic path lie on a plane normal to the pipe, and thus, no axial flow component contaminates the measured signal. Direct mode is used to measure the cross flow component, while multi-reflection mode is used to detect the swirl intensity. The performance characteristics of ultrasonic flow meters are investigated numerically using both analytical velocity profiles and CFD results for the flows downstream from the single elbow and double elbows out-of-plane. Results show that specially designed dual sensor ultrasonic flow meters could be useful in calibration facilities for in-situ diagnosis of swirl and cross flow in non-ideal installations.

## INTRODUCTION

Most industrial pipe flows are complex and non-uniform since it is seldom possible to make use of the long straight lengths of constant diameter pipe that are required to achieve fully developed ideal pipe flow. However, ideal pipe flow conditions are normally assumed for the design of flow meters and thus, the presence of secondary flows is known to cause significant metering inaccuracies [1,2]. As a result, the characteristics of non-ideal secondary flows are important to accurate flow measurement.

Identifying swirl and cross flow characteristics has been an important issue in attaining accurate flow measurement. A relationship between the meter factor and the swirl parameter has been suggested to correct the meter performance. Swirling flows are also often found in industrial applications where intense mixing is required. Hydrodynamic mixing is highly dependent on mixer design, which generates swirl and cross flows.

The rapid evolution of ultrasonic technology is offering prospects for improved flow metrology. With its non-intrusiveness, simple principle of operation, and relative easy design/implementation, ultrasonic flow meters have recently become popular. This trend is likely to continue given current advances in computing capabilities make the implementation of complex ultrasonic sensors ever more possible.

This paper describes ultrasonic flow measurements using dual-sensor, travel-time techniques. The objectives of this work are to understand and assess the prospects of ultrasonic technology for determining secondary flow characteristics and improving flow measurements by identifying and reducing errors caused by disturbances of the flow profile. The sensitivity to swirl in ultrasonic measurements is a disadvantage for practical flow measurement, but it can be useful for diagnosis of the disturbed secondary flows. This paper focuses on multi-reflection ultrasonic flow meters and their capabilities for measuring non-ideal secondary flow. When the sensors and the acoustic paths lie on a normal plane with respect to a pipe, none of the axial flow components contaminate the measured signal and secondary flow characteristics can be clearly detected.

 

## NOMENCLATURE

| | |
|---|---|
| $C$ | Speed of sound |
| D | Pipe Diameter |
| U , V , W | Flow velocities in the $X$ , $Y$ , and $Z$ directions |
| **V** | Fluid velocity |
| $V_I$ | Meter indicated velocity |
| $V_o$ | Taylor vortex strength |
| $V_s$ | Averaged fluid velocity along the path |
| $X, Y, Z$ | Cartesian coordinates |
| b | Chordal location |
| $d_c$ | Distance from a vortex center |
| $d_o$ | Taylor vortex core size |
| **e** | Unit vector along sound path |
| $\mathbf{e}_s$ | Unit vector along straight sound path |
| $\mathbf{e}_x, \mathbf{e}_y, \mathbf{e}_z$ | Direction cosines of ultrasonic path |
| $f_r(r)$ | Axisymmetric function |
| $f_\theta(\theta)$ | Angular function |
| $r_n$ | n-th reflection mode |
| $r, \theta$ | Polar coordinates |
| $r_v$ | $d_c/d_o$ |
| $s$ | Path length between the two sensors |
| $t$ | Travel time |
| α | Azimuthal angle |
| β | Arc angle of a chordal path |
| $\phi$ | Axial angle of a chordal path |

## BASIC ULTRASONIC FLOWMETER

Current ultrasonic flow metering technology benefits from simple design and ease of operation. A general description of ultrasonic metering can be found in reference [3]. Two common types of methods used for ultrasonic flow metering are travel-time and Doppler techniques. This paper describes ultrasonic flow measurements made using a single pair of dual-sensor, travel-time techniques. Travel-time ultrasonic flow meters measure the difference between the two opposite pulse propagation times along an ultrasonic path defined by the dual sensors. The basic equations for the propagation times can be written as:

$$\int_1^2 dt = t_{12} = \int_1^2 \frac{ds}{C + \mathbf{V} \cdot \mathbf{e}} \approx \frac{s}{C + V_s}$$
$$t_{21} = \int_1^2 \frac{ds}{C - \mathbf{V} \cdot \mathbf{e}} \approx \frac{s}{C - V_s} \qquad (1)$$

where 1 and 2 are the sensor locations, $t$ is the travel time, **V** is the fluid velocity, $C$ is speed of sound, **e** is a unit vector of sound path, $s$ is path length between the two sensors, and $V_s$ is the averaged fluid velocity along the path. Thus, from the above equations, we have

$$V_s = \frac{s}{2}\left(\frac{1}{t_{12}} - \frac{1}{t_{21}}\right) \quad \text{and} \quad C = \frac{s}{2}\left(\frac{1}{t_{12}} + \frac{1}{t_{21}}\right) \qquad (2)$$

The travel time and meter response will depend on the integration line of the acoustic propagation path, which is defined by the two sensors and the fluid medium; in general, the acoustic propagation path is not in a straight line. The effects of curved ray paths on meter performance has been investigated and reported in reference [4]. These showed that for most practical applications straight-line paths could be assumed. Although, the technique of ultrasonic flow metering can be applied to various pipe geometries, we have limited our study to meters used in circular pipes.

In this paper, a right-hand Cartesian coordinate system ( $X, Y, Z$ ) is used. The positive $Z$ direction is the flow direction; the positive $Y$ direction is upward; and the $X$ direction is to the right, looking upstream. U , V , and W are the flow velocities in the $X$ , $Y$ ,and $Z$ directions, respectively. All lengths are normalized by the pipe diameter, D .

As shown in previous studies [4], the configuration parameters for dual-sensor ultrasonic flow meters installed in circular pipes are the chordal location b , the path azimuthal angle α with respect to the $X$ direction, and the path axial angle, $\phi$ , with respect to the $Z$ direction. The chordal location can also be given by β , the arc angle of a chordal path, and their relationship is given by $b = \cos(\beta/2)/2$ . Referring to eqn. (1), the effective velocity seen by the flow meter is

$$V_s = \mathbf{V} \cdot \mathbf{e}_s = \mathrm{U}e_x + \mathrm{V}e_y + \mathrm{W}e_z \qquad (3)$$

where $\mathbf{e}_s$ is a unit vector of straight sound path, and $e_x = \cos(\alpha)$ , $e_y = \sin(\alpha)$ , and $e_z = \cos(\phi)$ are the direction cosines of ultrasonic path in the $X$ , $Y$ , and $Z$ directions, respectively. A meter indicated velocity $V_I$ is normally given by $V_I = V_s / e_z = V_s / \cos(\phi)$ to represent an averaged axial velocity.

## MULTI-REFLECTION ARRANGEMENTS

At its most simple configuration, a dual-sensor, travel-time ultrasonic flow meter requires only two sensors. These sensors can be placed anywhere in the pipe, as long as they can communicate with each other. The sound path between the sensors can follow a single segment in direct mode or multi-segments in reflective mode.

Figure 1 shows schematic diagrams of generic multi-reflection ultrasonic flow meters in a circular pipe. Several special cases are shown: (1) direct mode or zero reflection mode ( $r_0$ ); (2) diametric single reflection mode ( $r_1$ ); (3) triangular double reflection mode ( $r_2$ ); and (4) triple reflection mode ( $r_3$ ). Multi-reflection meters make use of multiple direct mode segments in a sound path. The total number of segments equals the number of reflections plus the initial segment. In general, each segment can have its own path parameters ( $\alpha$ , $\beta$ and $\phi$ ).

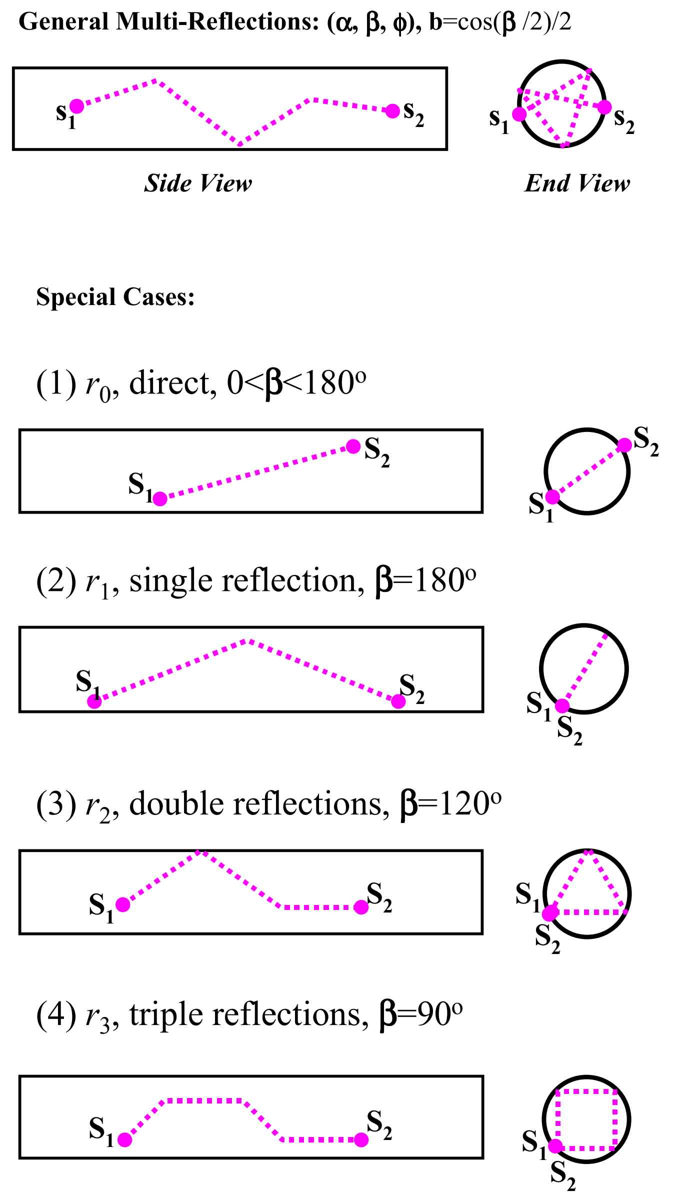


**Figure 1. Schematic diagram of multi-reflection dual-sensor ultrasonic flow meters.**

Although the surface of the pipe can be specially designed for controlling the reflection direction of each path, the natural reflection angle produced from the circular pipe surface is here assumed for all reflections. In multi-reflection paths, this leads to equal values for the arc angle ( $\beta$ ), path angle ( $\phi$ ), chordal path length ( $s$ ), and chordal radial offset ( $b$ ) for all segments. However, the path angle, $\alpha$ , will be different for each segment with a unique relationship given by the reflection rule. In this paper, unless otherwise indicated, $\alpha$ is meant to indicate the path angle for the first segment of a path. In addition, as shown in Figure 1 and excluding the direct mode, the same azimuthal angle location is selected for both transmission and receiving sensors. Thus the value of the arc angle for each segment is given by $\beta = 360/(r+1)$ degrees, where $r$ is the number of reflections. The direct mode sensor can be considered as a special case of a multi-reflection meter where $r = 0$ .

The effective velocity seen by a multi-reflection meter is equivalent to the average of the average velocities in all segments of the path. Since all segments have the same path length, the effective velocity for a $r$-reflection meter can be expressed as

$$\mathrm{V}_S = \sum_{r+1} (\mathrm{U}e_x + \mathrm{V}e_y + \mathrm{W}e_z)/(r+1) \qquad (4)$$

As with the direct mode meter, the indicated axial velocity $\mathrm{V_I}$ for multi-reflection meters is usually given by $\mathrm{V_I} = \mathrm{V}_s/\mathrm{e}_z$ . This can be done because there is only one axial angle $\phi$ and thus, only one $\mathrm{e}_z$ for all segments in a multi-reflection meter.

## SELECTED PIPEFLOW PROFILES.

The numerical simulation of a ultrasonic flow meter performance requires a complete 3-D pipe flow field and its gradients in all three directions (that is, if ray theory is used to determine the propagation path). Various pipeflow velocity profiles can be selected to test the sensitivity of the design to velocity profile induced effects and to investigate the resulting performance of a dual-sensor meter.

Analytical velocity profiles and computational fluid dynamic (CFD) results for common industrial pipe flow are used here. Using the first approach, a quasi-realistic velocity profile is obtained by the superimposing of various simple analytical functions. Using this method, one can formulate a large number of artificial flow profiles by adding analytical functions that resemble various flow disturbances. The technique has been successfully used to ascertain the uncertainties of point-velocity integration methods for determination of volumetric flow rate [5] and to estimate the sensitivity of ultrasonic flow meters [4]. The method is not only a simple and economical way to construct complicate velocity profiles, but it also provides ways to study the effects of special flow fields similar to those encountered in generic flow meter installations and test meters.

A complete velocity field consists of three components: $\mathrm{U}$ , $\mathrm{V}$ , and $\mathrm{W}$ , and in general, the profiles are not axisymmetric. Many axial velocity profiles can be expressed as:

$$\mathrm{W}(x,y) = \mathrm{W}(r,\theta) = \mathrm{f_r}(r)\mathrm{f}_\theta(\theta) \qquad (5)$$

where $\mathrm{W}(r,\theta)$ is W given in polar coordinates. Table 1 shows some axisymmetric axial velocity functions, $\mathrm{f_r}(r)$ , while Table 2 shows some lists of angular functions $\mathrm{f}_\theta(\theta)$ .

In additional to the axial velocity component, the cross flow components U and V are also simulated. The classic

Taylor vortex model [7] can describe typical cross or swirl flows,

$$V_\theta = V_o r_v \exp(-r_v^2) \qquad (6)$$

Where $r_v = d_c/d_o$ and $d_c$ is the distance from the vortex center; $V_o$ and $d_o$ are the vortex constants for intensity and core size, respectively. This distribution does not directly exhibit the velocity variation that is inverse with the radius $d_c$. Instead, it gives more emphasis to the solid body rotation near the axis of rotation and to the exponential decay further from the center – characteristics that more closely resemble the features of vortices in pipe flows [8]. Another type of simulated cross flow used here is $U = 0.1\cos(r)$ or $V = 0.1\cos(r)$.

| ID | $f_r(r)$ |
|---|---|
| **UN** | 1, uniform |
| **LA** | $2(1-(2r)^2)$, laminar |
| **BM** | Given by Bogue and Metzner[6] |
| PL | $4(p+1)(p+2)(1-2r)^p$, Power Law |
| fr1 | $4(p+1)(p+2)(p+3)r(1-2r)^p$, slow core |
| fr2 | $8(p+1)..(p+4)\, r^2(1-2r)^p/3$, slow core |
| fr3 | $4(p=1)...(p+5)\, r^3(1-2r)^p/3$, slow core |
| fr4 | $\pi/(1/2-1/\pi)\cos(\pi r)$ |
| fr5 | $\pi/(1/4-2/\pi^2)\, r\cos(\pi r)$ |

**Table 1. Axial symmetric functions, $f_r(r)$.**

| ID | $f_\theta(\theta)$ |
|---|---|
| fθ0 | $1/2\pi$, uniform |
| fθ1 | $3\theta^2/2\pi^3$ |
| fθ2 | $\cos(\theta)/\pi$ |
| fθ3 | $\cos^2(\theta)/\pi$ |
| fθ4 | $\theta\cos(\theta)/2\pi$ |
| fθ5 | $\theta\cos^2(\theta)/2\pi$ |
| fθ6 | $\theta^2\cos^2(\theta)/\pi(\pi^2/3+1/2)$ |
| fθ7 | $e^{-a\theta}\cos(\theta)(a^2+1)/a(e^{-a\pi}-e^{a\pi})$ |
| fθ8 | $e^{-a\theta}\cos^2(\theta)a(a^2+4)/(a^2+2)(e^{a\pi}-e^{-a\pi})$ |
| fθ9 | $\cos^2(\theta/2)/\pi$ |
| fθ10 | $\theta\cos(\theta/2)/\pi$ |
| fθ11 | $(\theta^2-1)\cos^2(\theta)/\pi(\pi^2/3-1/2)$ |
| fθ12 | $(\pi+\theta)^2(\pi-\theta)^2 15/16\pi^5$ |

**Table 2. Angular functions $f_\theta(\theta), -\pi < \theta < \pi$.**

Based on these simple analytical velocity profiles, many complicated velocity fields can be formed. Table 3 shows some selected velocity fields used in this work. In the table, **PL** is a symmetric power law flow; **CRU** is a cross flow for U component; **1ed** is a single swirl eddy at pipe center line; **2edx** is two swirl eddies located at $(+x, y)$; **SNL** is a combination of two swirl eddies, uniform axial flow, and skewed axial flow normal to the plane of the eddies. The **SNL** profile is intended to simulate a single elbow flow. The **DBL** profile simulates a double-elbow flow and is a combination of a swirl eddy, a power law (**PL**), and a slow core flow (fr2). In all cases, unit vortex intensity is assumed, i.e., $V_o = 1$.

To investigate meter performance in a more conventional, non-ideal turbulent pipe flows, CFD models of the flow through a single elbow and double elbows out of plane were produced using a commercially available computer code. In Table 3, **LY** and **LXY** denote the single elbow and the double elbows CFD data, respectively.

| ID | Velocity profiles |
|---|---|
| **PL** | U=V=0, W= PL , power law |
| **CRU** | U=0.1cos(r), V=0, W=1 |
| **1ed** | 1 vortex at (0,0) with $r_o$=0.25 and W=1 |
| **2edx** | 2 vortices at (±0.15,0) with $r_o$=0.15 and W=1 |
| **SNL** | 2 vortices at (±0.15,0.1) with $r_o$=0.15, W=1-0.2fr1*fθ2 with 90° shifted in θ. |
| **DBL** | 1 vortex at (0,0) with $r_o$=0.25, W=0.9PL+0.1fr2 |
| **SKX** | U=V=0, W=1+fr1*fθ2, skew in x direction |
| **LY** | Single elbow CFD |
| **LXY** | Double elbows out of plane CFD |

**Table 3 Selected velocity flow fields. The vortex centers are given in $(x,y)$ coordinates.**

## RESULTS

As indicated above, ultrasonic flow meter performance depends on sensor location ($\alpha$, $\phi$, and $b$) and these sensors can be specifically designed to measure different flow characteristics.

*A. A sensor for flow rate measurements.*

When the determination of the flow rate is the primary interest (most common use of this type of sensors), the sound path is set to have an incline angle of $\phi$ with respect to the pipe axial direction. The meter indicated axial velocity $V_I$ is given by $V_I = V_s/e_z = V_s/\cos(\phi)$. The next few figures show the results of this type of meter. Figure 2 shows the profile effects on direct mode dual-sensor meter installations as a function of the α. In the plot, the average velocity normalizes the indicated velocity. That is, the value of 1.0 for the indicated velocity means that the meter measures a correct average flow. The deviation from the value of 1.0 indicates the amount the meter misinterprets from the actual flow due to the profile effects. Since the effective velocity seen by the meter contains a cross flow velocity component as shown in eqn.(3), the indicated velocity $V_I$ is contaminated by the non-ideal secondary cross-flow velocities and thus the measured result could yield a flow rate with significant different from the actual flow.

The effect of secondary flows on dual sensor flow meters has been the subject of many studies [4]. As suggested by these studies, the indicated velocity for direct mode, dual-sensor flow meters is constant in axisymmetric flows such as **PL** and **1ed** flows. However, it is worth noting that values are equal to 1.0 for both the single swirl (**1ed**) and the skew (**SKX**) flows. There are no angular effects on the indicated velocity for the skew flow; however, the double swirl profiles produce large α angle variations in meter indication. The CFD data shown for the single elbow LY is for Z=10 and for the double elbow out of plane LXY is for Z=20. More data for other locations are shown on figs 7 and 8 below. The effects of a single elbow flow are similar to those of double swirl flows. The measured velocity ranges from 0.91 to 1.05. The general feature of the double elbow out of plane is similar to that of a single swirl flow superimposed on an axisymmetric axial flow. Although the indicated velocity is significantly different from the true flow rate of 1.0, its angular effect is relatively small for the double elbow flows. The cross flow effect on the meter output is also seeing in the **CRU** flow.

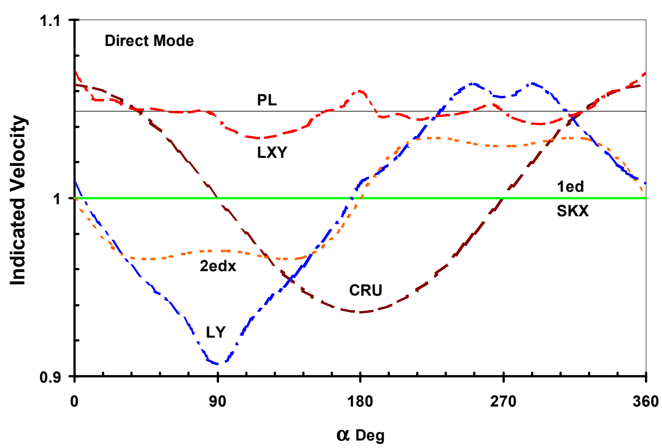


**Figure 2. Meter indicated velocity for an inclined dual-sensor ultrasonic flow meter in various velocity profiles (b = 0, ϕ = 45°). LY is for Z = 10; Lxy is for Z=20. (Values for SNL and DBL are not shown for clarity)**

Among the three velocity components, the axial component, W, is normally the one desired to be measured, while the cross components; U and V could contribute to flow meter error. When flow rate is the desired quantity, the cross-flow sensitivity should be minimized. Both multi-path or multi-reflection techniques can be used to increase the accuracy of a flow meter or to minimize the cross-flow sensitivity. The results of the meter-indicated velocities for inclined dual-sensor flow meters in various velocity profiles are shown in Figures 3 and 4 for a single-reflection mode and a double-reflection mode, respectively. For multi-reflection meters, since $e_z$ is a constant value as shown in Eqn. (4), the result is averaged over all path segments due to the axial component W. However, some of the cross components U and V are cancelled among segments due to the fact that the vales of directional cosines $e_x$ and $e_y$ are different for different segments. The degree of cancellation or addition on the cross flow component depends on the meter design and type of flow. For flow rate measurement, the cancellation of the cross flow component will result in less sensitivity in flow meter installation effects, while the additional effects can be used for measuring the swirl and cross components.

Figure 3 shows that the angular effects of the indicated velocity for single-reflection meters are small for all flows tested. This allows that single reflection meters to eliminate the cross flow effects very effectively. As seen, the indicated velocity is 1.0 for **1ed**, **2edx**, **CRU**, **SKX**, and **SNL** flows and it is very insensitive to the angular position for **PL**, **LY**, **LXY** and **DBL** flows. This trend indicates a single-reflection meter can be used to improve flow measurements in flow fields having cross and swirl velocity components. However, its benefit on axial component measurements is limited as shown in the results for **DBL**, **LXY** and **PL** flows.

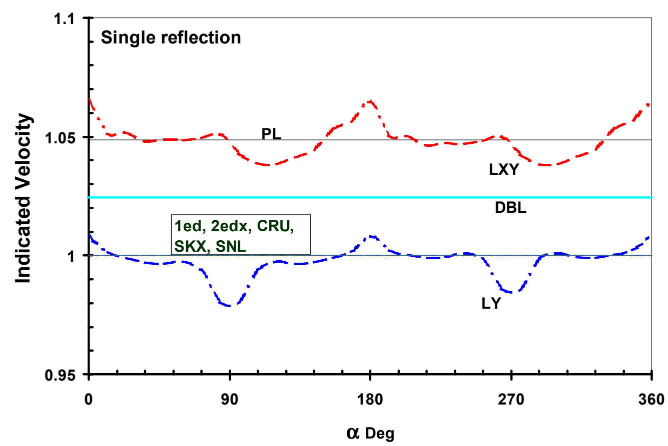


**Figure 3. Meter indicated velocity for a single reflection, inclined dual sensor ultrasonic flow meter in various velocity profiles (b = 0 and ϕ = 45°). LY is for Z = 10; Lxy is for Z=20.**

The results in Figure 4 show that the double reflection arrangements do not significantly improve the accuracy of a flow meter, except by providing a better velocity average due to a larger averaged domain. In fact, they will produce more errors in some cases where flow swirl flows exist, such as those of **LXY** and **1ed** flows. The results also show that these indicated velocities are different from those obtained by the direct and single-reflection modes. These results indicate that installation location and orientation might be critical to satisfactory levels of meter performance, and special caution is needed whenever this class of meters is used to measure flow rate in the presence of cross flows.

 

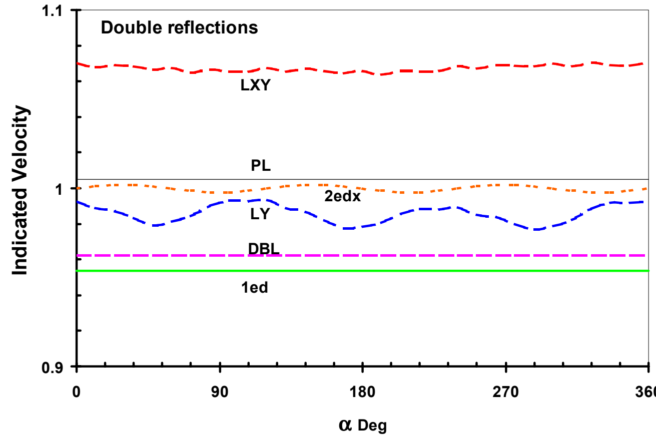


**Figure 4. Meter indicated velocity for a double reflection, inclined dual sensor ultrasonic flow meter (b=0 and $\phi$=45$^o$). Values=1.0 for CRU and SKX. The value of SNL is close to that of 2edx. LY is for Z = 10; Lxy is for Z=20.**

*B. Special flow meters for cross and swirl measurements*

The discussion above considered flow meters commonly used for flow rate measurements. These flow meters have sensors located in both downstream and upstream positions. In this section, we shall discuss special multi-reflection meters and their application for measuring secondary flow field properties, generally known to consist of swirl and cross components.

Swirling flows are also often found in industrial flow applications when intense mixing is required, thus identifying these secondary flow characteristics has been an important issue in accurate flow measurement. As previously discussed, the sensitivity to swirl of an ultrasonic measurements is a disadvantage for practical flow measurement, but can be useful for the diagnosis of disturbed secondary flows. When the sensors and the acoustic path lie on a normal plane with respect to the pipe (i.e. $\phi = 90^o$), no contamination of the axial flow component is measured in the signal. Thus, secondary flow characteristics can be clearly detected.

Special attention should be paid to the possibility of using different path arrangements to determine the degree of swirl and cross-flows. A direct mode can be used for cross-flow measurements, while a triangular double-reflection mode can be used for swirl flow measurements. It is noted that a single-reflection mode will show zero output for all flows, and thus, will not be useful.

Figure 5 shows cross-flow intensity in various flow profiles, as measured by a special direct mode, dual-sensor ultrasonic flow meter ($\phi = 90^o$). The cross flow meter detects only the averaged cross-flow velocities in the direction of the meter path. No effect of axial velocity distribution is shown on the output of the meter. As expected, the cross velocities for **SKX** and **PL** are all zero, since there are no cross components in the flow fields. However, it is worth noting that the measured cross velocities for **1ed** and **DBL** are also zero, even if the swirl is present in these flow fields. Figure 6 shows the swirl velocity measured by a special dual-sensor, double-reflection ultrasonic flow meter ($\phi = 90^o$) in various flow profiles. Again, the axial velocity component has no contribution to the output of the swirl meter. The meter effectively detects the swirl intensities for **LXY**, **1ed** and **DBL**. The measured swirl intensity is zero for **PL**, **CRU**, and **SKX** flows, and is very small for **LY** and **2edx** flows. The swirl for SNL is very close to that of 2edx and is not shown for clarity.

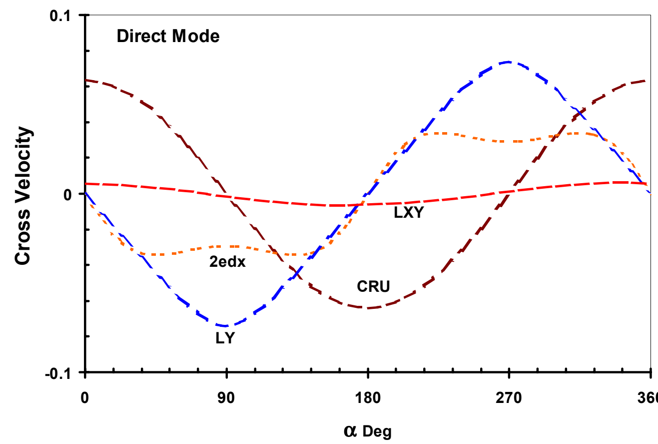


**Figure 5. Cross-flow intensity in various flow profiles as measured by a special direct mode dual-sensor ultrasonic flow meter ($\phi$ = 90$^o$). Cross Velocity = 0 for 1ed, SKX, DBL, and PL, and the value for SNL is similar to that of 2edx. LY is for Z = 10; Lxy is for Z=20.**

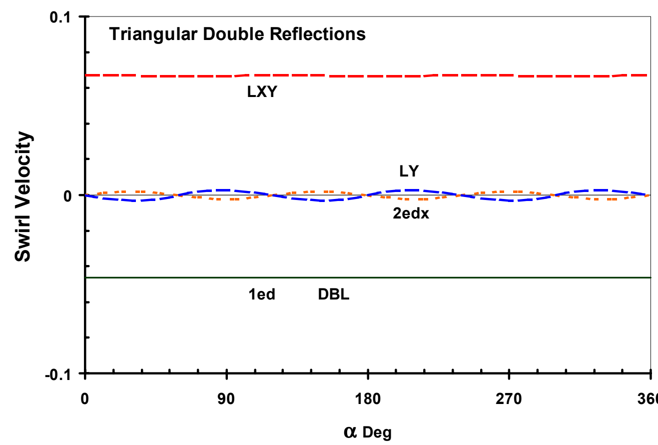


**Figure 6. Circulation intensity, denoted by the swirl velocity, in various flow profiles as measured by a special dual-sensor double reflection ultrasonic flow meter ($\phi$ = 90$^o$). Swirl = 0 for PL, CRU and SKX. LY is for Z = 10; Lxy is for Z=20.**

These special meters can be used to detect the decay of the secondary flows downstream of elbows. The decay of the cross-velocity of the single elbow flow, **LY**, produced by CFD as measured by a direct mode, cross-flow meter is shown in Figure 7. The decay of swirl velocity in the double elbow out of plane, **LXY**, as measured by a triangular double reflection swirl meter, is shown in Figure 8. The angular dependence of the cross velocity is clearly shown for the single-elbow flow. Although the swirl intensity of the double-elbow flow decreases as it moves downstream, the swirl intensity is essentially independent of the angular location. The results suggest that a concentrated, single-swirl eddy can simulate the double-elbow flow. The cross-flow velocity near the single elbow (Z = 5), as shown in Fig.7, varies from a minimum of -0.11 (near $\alpha = 90^o$), to a maximum of +0.11 (near $\alpha = 270^o$). The results show that the elbow flows are not fully developed, even at Z = 55 for the single elbow and at Z = 80 for the double elbow out of plane.

These results suggest that the special meters can be used in-situ to detect and monitor and diagnoses secondary flow and swirl and cross flows in non-ideal installations. The ability of an in-situ diagnosis of secondary flows is an important component in a calibration facility. For a flow calibration facility to be classified as a standard, it must constantly undergo rigorous evaluations to confirm that the flow field is a good, ideal flow. Not only should a good flow facility require an accurate average flow rate determination, but it should also be able to maintain and characterize various flow field properties. For example, if skew and swirl velocity components exist in a calibration system, significant errors on meter calibration can occur.

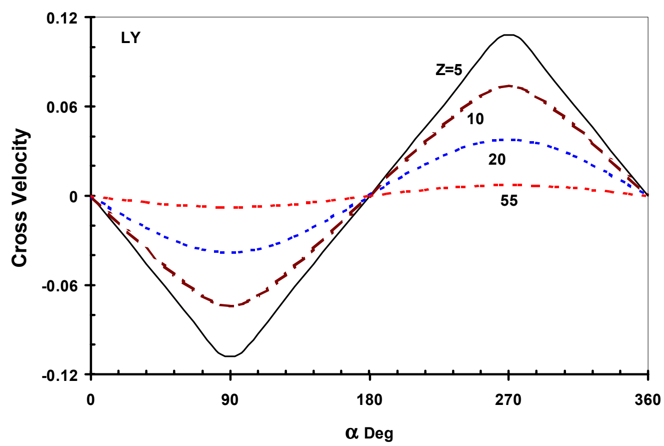


**Figure 7. Cross flow intensity of a single elbow flow as measured by a special direct mode cross flow meter ($\phi = 90^o$).**

Traditionally, flow calibration facilities have relied on the assumption that the flow fields produced by the facilities are ideal, fully developed pipe flows. Research has shown that deviations from this assumption can lead to significant errors in meter calibration, even when these calibration systems typically provide good average flow rate determinations. Although the flow profile of a calibration facility can be evaluated by experimental means, the high cost of a traditional evaluation and the fact that the data obtained only relates to the condition at the time of the evaluation and not at the time of calibration, makes the use of in-situ secondary flow detectors attractive.

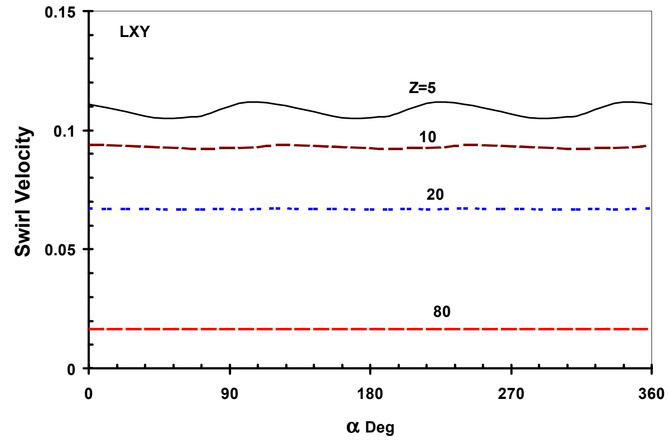


**Figure 8. Swirl intensity of double elbow out-of-plane flow as measured by a special double reflection swirl meter ($\phi = 90^o$).**

## SUMMARY

Dual-sensor, travel-time ultrasonic flow meters have been modeled numerically in a wide range of flow conditions. Performance prospects of acoustic flow meters were investigated for pipe flows for both analytical velocity profiles and common industrial pipe flows. Various analytical pipe flow velocity profiles were selected to test the sensitivity to secondary flow effects. CFD results for flows from single elbow and double elbows out-of-plane are also used. These results show that specially designed, dual-sensor ultrasonic flow meters can be used for in-situ diagnosis of swirl and cross flows in non-ideal installations.

The three-sensor pair ultrasonic flow meter as shown in Fig. 9 is an example of a meter able to provide in-situ diagnosis of swirl and cross flow in calibration facilities. It consists of two direct-mode, cross-flow sensors (located 90 degrees apart and able to detect the cross-flow component), and one triangular double-reflection sensor used to detect the swirl flow. In addition to being used as a flow diagnostic tool, cross and swirl sensors could prove beneficial in field applications where installation effects can lead to gross errors when ultrasonic signals are evaluated using conventional integration. By knowing the characteristics of non-ideal, swirl and cross flow components in pipes and understanding the nature of the installed ultrasonic techniques, it could be feasible to significantly improve metering performance.

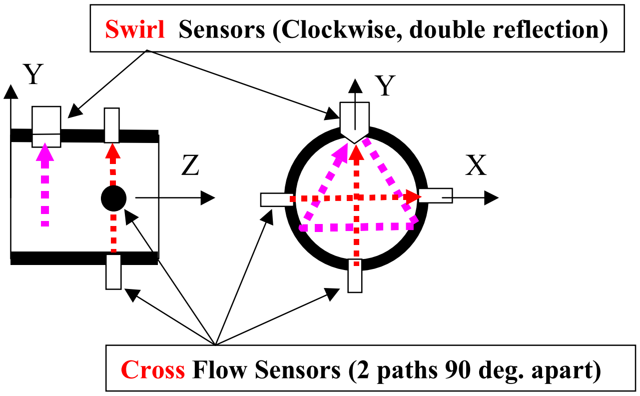


**Figure 9. Special swirl and cross flow meters ($\phi = 90^o$).**

## ACKNOWLEDGMENTS

The technical contributions of our Fluid Flow Group colleagues, Dr. G. E. Mattingly and Mr. J. D. Wright are gratefully acknowledged.

## REFERENCES

[1] Mattingly, G. E. and Yeh, T. T., 1988, "Flow meter Installation Effects," Proc. National Conference of Standards Laboratories Annual Conference, Wash., DC, Aug. 14-18, 1988, published by NCSL, Boulder, Co.

[2] Mattingly, G. E. and Yeh, T. T., 1992, "Flow meter Installation Effects Due to Several Elbow Configurations," *Proceedings of the 2nd International Symposium on Fluid Flow Measurement*, pp. 271-283.

[3] Lynnworth, L. C. 1989, "Ultrasonic Measurements for Process Control," Academic Press, San Diego, CA .

[4] Yeh, T. T. and Mattingly, G. E., 1997,"Computer Simulations of Ultrasonic Flow Meter Performance in Ideal and Non-ideal Pipeflows," Procs. ASME Summer Mtg., Vancouver, Canada.

[5] Salami, L. A., 1971, "Errors in the velocity-area method of measuring asymmetric flows in circular pipes," International Conference on Modern Developments in Flow Measurement, A.E.R.E. and NEL, Harwell, UK, Paper No. 31.

[6] Bogue, D. C. and Metzner, A. B., 1963, "Velocity Profiles in Turbulent Pipe Flow," *I&EC Fundamentals*, Vol. 2, No. 2.

[7] Dryden, H., Murnaighan, F. D. and Bateman, H., 1956, "Hydrodynamics," *Dover Publ. Co.*, New York, NY, P.213.

[8] Mattingly, G. E. and Yeh, T. T., 1988, "NIST's Industry-Government Consortium Research Program on Flow Meter Installation Effects: Summary Report for Research Period July - December, 1987," *NISTIR* 88-3898.